BioMetals 1992, **5**, 141–148

Stereochemical characterization of rhizoferrin and identification of its dehydration products

Hartmut Drechsel, Günther Jung & Günther Winkelmann*

*Institut für Organische Chemie and *Institut für Biologie, Mikrobiologie & Biotechnologie, Universität Tübingen, Tübingen, Germany*

Received 20 June 1992; accepted for publication 26 June 1992

The polycarboxylate siderophore, rhizoferrin, and its dehydration products were separated by preparative HPLC and characterized by ^{13}C-NMR, ^{1}H-NMR, UV, circular dichroism (CD) and IR spectroscopy, and also by capillary electrophoresis. Assignment of all carbon atoms and protons by NMR spectra confirmed the structure of rhizoferrin and gave evidence for the presence of the cyclized dehydration byproducts, imidorhizoferrin and bis-imidorhizoferrin. The imido forms were also characterized by their mobility during capillary electrophoresis. UV spectra revealed a 1:1 iron:ligand ratio above pH 3. Based on the absorption maximum of the metal ligand charge transfer band at 335 nm a molar extinction coefficient of 2300 M^{-1} cm^{-1} was calculated for ferric rhizoferrin. CD measurements revealed that the quarternary carbon atoms of the two citric acid residues possess an *R,R* configuration and that the iron complex of rhizoferrin adopts a Λ configuration around the metal center.

Keywords: imidorhizoferrin, iron complex, iron transport, rhizoferrin, siderophores

Introduction

Rhizoferrin is a polycarboxylate or complexone type siderophore which was originally isolated from low-iron cultures of the fungus *Rhizopus microsporus* var. *rhizopodiformis* (Drechsel *et al.* 1991). Later it was shown that rhizoferrin is widespread in fungi belonging to the Mucorales and Entomophthorales within the Zygomycetes (Thieken & Winkelmann 1992). Most other fungi of the Ascomycetes and Basidiomycetes are known to produce hydroxamate type siderophones; however, the Zygomycetes are the only fungal group known so far which synthesize polycarboxylate type siderophores (Winkelmann 1992).

Although the structure of rhizoferrin has already been elucidated by our group (Drechsel *et al.* 1991), the present study provides further structural and configurational data of rhizoferrin and, especially, of its dehydration products.

Address for correspondence: G. Winkelmann, Mikrobiologie/Biotechnologie, Auf der Morgenstelle 1, 7400 Tübingen, Germany.

Materials and methods

Strains and growth conditions

The following strains were used for the production of rhizoferrin: *Rh. microsporus* var. *rhizopodiformis*, *Rh. arrhizus* (previously named *Rh. oryzae*) and *Cunninghamella elegans*. All were kindly provided by Dr J. Boelaert (Brugge, Belgium).

Isolation of rhizoferrin

Rhizoferrin was isolated from low-iron culture filtrates as described recently (Drechsel *et al.* 1991). Briefly, the culture filtrate was first passed through a cation exchange column. After adjusting the pH to 6.8 the efluent was subsequently passed through an anion exchange column (formate form). The bound anions were then eluted with 60% formic acid, concentrated by evaporation and separated on a Biogel P2 column. Fractions which gave a positive reaction on chrome azurol S plates were collected and lyophilized. According to analytical HPLC the purity of rhizoferrin was greater than 95%.

Analytical and preparative HPLC

Analytical separation of rhizoferrin was performed on a C_{18} reversed-phase column (Nucleosil, 5 μm, 250 ×

4.6 mm) using a gradient of acetonitrile in water (3–8%) plus 0.1% trifluoroacetic acid (Shimadzu LC-9A, equipped with an integrator C-R4AX, gradient controller SCL-6B and automatic sampler SIL-6B). Preparative HPLC was performed on a Nucleosil C_{18} column (250 × 20 mm, 5 μm) using a flow rate of 10 ml min^{-1} and a gradient of 3–10% acetonitrile in water plus 0.1% trifluoroacetic acid within 20 min. Approximately 10 mg crude rhizoferrin in 150 μl of water was injected for each run. Siderophore positive fractions were collected and lyophilized, yielding a colorless, fluffy compound.

Capillary electrophoresis

Capillary electrophoresis was performed with an ABI 270A HT capillary electrophoresis system equipped with an autosampler (Applied Biosystems Inc.). Samples were injected in a 72 cm fused silica capillary coated with 'microcoat' (Applied Biosystems Inc.) and run with −15 kV in a buffer of 20 mM citric acid (pH 2.5).

Mass spectra

Ion spray mass spectra were recorded via direct injection of sidereophore solutions on a Sciex API III triple–quadrupole mass spectrometer with 2400 Da mass range equipped with an ion spray ion source (Sciex, Toronto, Canada), as described in a previous paper (Drechsel *et al.* 1991).

NMR spectra

^{1}H-NMR and ^{13}C-NMR spectra were recorded on a Bruker AC 250 instrument at 250 MHz (^{1}H resonance) in D_2O at 305 K. Assignments were made by comparison with known compounds. Chemical shifts of both ^{1}H and ^{13}C refer to 3-(trimethylsilyl)-propionic acid-2,2,3,3 d_4-sodium salt.

UV spectra

UV spectra were recorded on a Hewlett-Packard diode array spectrometer HP 8452 A, connected to an HP Vectra QS/16S with an acquisition time of 5 s over a range of 190–600 nm for the ferric forms and 25 s over a range of 190–350 nm for the free ligands. Samples (1.5×10^{-4} M) were dissolved in bidistilled water and the solutions measured in quartz cuvettes with a path length of 1 cm at a temperature of 22 °C.

Circular dichroism (CD) spectra

CD spectra were recorded on a Jasco 720 CD spectrometer (Japan Spectroscopic Company Ltd, Tokyo, Japan) equipped with IBM compatible PC for data acquisition and processing. Recording conditions and samples were according to those for UV spectroscopy.

IR spectra

IR spectra were recorded on a Bruker IFS 48 Fourier transform (FT) IR spectrometer. The samples were measured as KBr pellets with a resolution of 2 cm^{-1}.

Results

NMR studies

Rhizoferrin (**I**) and its accompanying byproducts (**II** & **III**; Figure 1) were isolated by preparative HPLC resulting in a main rhizoferrin fraction and two minor fractions which eluted at higher retention times (Figure 2). The first two fractions containing compounds **I** and **II** were collected, lyophilized and used for spectroscopic characterization. The ^{13}C-NMR spectrum of rhizoferrin (**I**; Figure 3a) shows resonances of eight carbon atoms according to the numbering in Figure 1. The assignment of carbons is summarized in Table 1. Thus, the structure of rhizoferrin as described in our previous paper (Drechsel *et al.* 1991) could be fully confirmed.

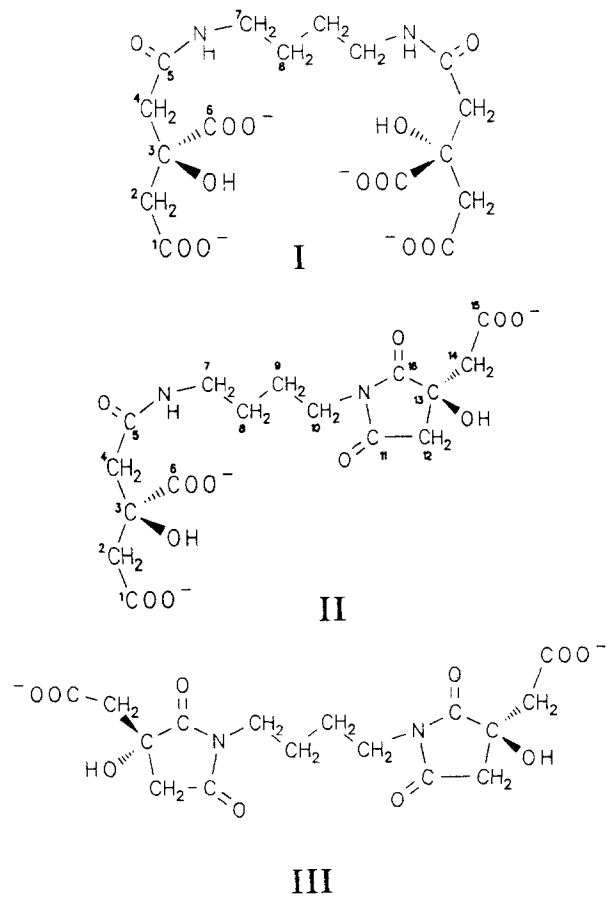

Figure 1. Structural formulae of rhizoferrin (**I**), imidorhizoferrin (**II**) and bis-imidorhizoferrin (**III**).

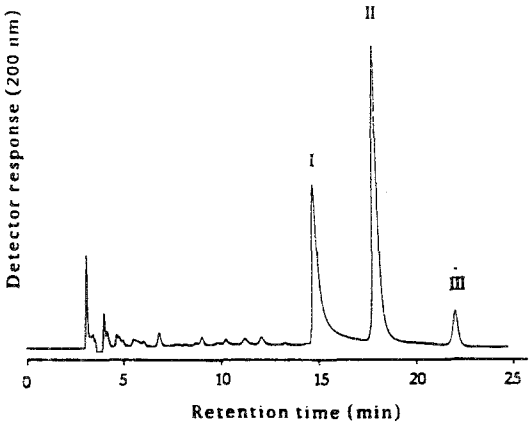

Figure 2. HPLC separation of rhizoferrin (**I**), imidorhizoferrin (**II**) and bis-imidorhizoferrin (**III**) on an analytical column (Nucleosil C_{18}, 5 μm, 250 × 4.6 mm) using a 3–8% gradient of acetonitrile in water plus 0.1% trifluroacetic acid.

Moreover, HPLC on-line ion spray mass spectra of the second HPLC peak (Figure 2) revealed a mass of 418, suggesting the loss of a water molecule. ^{13}C-NMR and ^{1}H-NMR (Figure 3; Tables 1 & 2) allowed us to distinguish between a dehydration to aconitic acid and a cyclized imido derivative (**II**). Signals of unsaturated fragments could not be detected in the ^{13}C-NMR or ^{1}H-NMR spectra, excluding the formation of an unsaturated bond as found in aconitic acid. In the ^{1}H-NMR spectrum the signals belonging to the citric acid residues doubled up in the case of the dehydration product (**II**), suggesting a cyclization of one citric acid residue into a succinimide derivative. The two triplet signals from the methylene protons of the diamino bridge also doubled into four multiplet groups due to the loss of symmetry. Likewise the eight ^{13}C signals of rhizoferrin doubled pairwise into 16 distinguishable carbons, suggesting that the dehydration product represents a unilaterally cyclized imido derivative, named imidorhizoferrin.

Capillary electrophoresis

Isolated compounds exhibiting uniform HPLC peaks were further analyzed by capillary electrophoresis using fused silica capillaries with a buffer of 20 mM citric acid, pH 2.5 and 15 kV, polarity negative at inlet side and detection wavelength 200 nm (Figure 4). Under these conditions a neutral marker (mesityl oxide) appears at the detector after 8.5–9 min, depending on the coating. Analytes having a net negative charge at the buffer pH migrate faster compared with the neutral marker; positively charged compounds appear later. The existence of

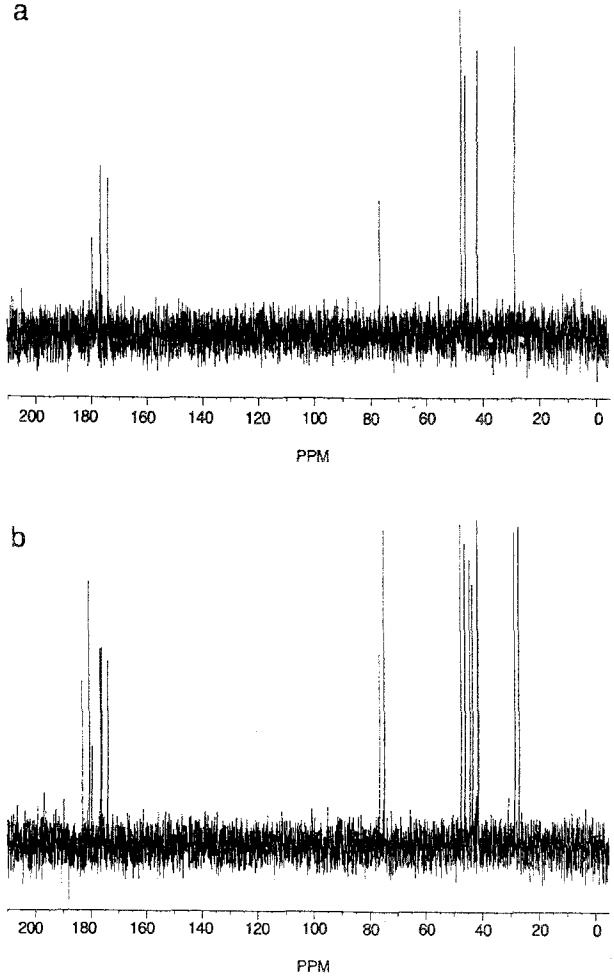

Figure 3. ^{13}C-NMR spectra of (**a**) rhizoferrin (**I**) and (**b**) imidorhizoferrin (**II**).

both imidorhizoferrin (**II**) and bis-imidorhizoferrin (**III**) was additionally confirmed in their electrophoretic behavior during capillary electrophoresis, as imidorhizoferrin and bis-imidorhizoferrin have lost one or two negative charges, respectively. Rhizoferrin and its dehydration products possess different numbers of carboxylate groups at pH 2.5. Therefore, rhizoferrin (**I**) migrates ahead of imidorhizoferrin (**II**) and bis-imidorhizoferrin (**III**) to the positive side. Figure 4a shows a purified extract containing mainly rhizoferrin and small amounts of imidorhizoferrin. Figure 4b shows the same compound after 1 day of incubation in 20 mM citric acid buffer, pH 2.5 at 20 °C, showing increased formation of the mono-imido form. Figure 4c finally shows an imidorhizoferrin fraction after 1 day of incubation in acidic medium showing larger amounts of bis-imidorhizoferrin (**III**). Thus, prolonged exposure of rhizoferrin at pH 2.5 resulted in a marked alteration of

Table 1. ^{13}C-NMR data of rhizoferrin and its cyclic dehydration product

Carbon no.[a]	Rhizoferrin		Imidorhizoferrin	
	p.p.m.	assignment	p.p.m.	assignment
16			182.9	Cit–C_q–CONH (ring)
11			180.3	Cit–CH_2–Co (ring)
6	179.3	COOH of C quart.	179.3	
1	176.2	COOH terminal	176.3	
15			175.8	Cit–COOH (terminal, ring)
5	173.6	CONH	173.7	
3	76.3	C quart. of citric acid	76.4	
13			74.7	C quart. (ring)
4	47.3	Cit–CH_2–CONH	47.3	
2	45.8	Cit–CH_2–COOH	45.8	
14			44.1	Cit–CH_2–COOH (bonded to ring)
12			43.2	Cit–CH_2–CO–N (ring)
7	41.5	CH_2NH–	41.3	
10			41.2	CH_2–$N(CO)_2$
8	28.3	CH_2CH_2NH–	28.3	
9			26.7	CH_2–CH_2–$N(CO)_2$

[a]Numbering of carbon atoms as in Figure 1.

Table 2. ^{1}H-NMR data of rhizoferrin and its cyclic dehydration product

Carbon no.[a]	Rhizoferrin			Imidorhizoferrin		
	p.p.m.	assignment	*J* (Hz)	p.p.m.	assignment	*J* (Hz)
10				3.41 (*t*)	$CH_2N(CO)_2$	6.7
14				3.09	Cit–CH_2 (2aa)	18.7
7	3.02 (m)	CH_2NH		3.05 (*t*)	CH_2NHCO	6.6
14				3.01	Cit–CH_2 (2aa)	18.7
12				3.00	Cit–CH_2 (2ba)	19.3
4	2.95	Cit–CH_2 (aa)	16.1	2.95	Cit–CH_2 (1aa)	16.1
14				2.94	Cit–CH_2 (2ab)	19.7
12				2.93	Cit–CH_2 (2ba)	19.3
4	2.88	Cit–CH_2 (aa)	16.1	2.89	Cit–CH_2 (1aa)	16.1
14				2.86	Cit–CH_2 (2ab)	19.7
12				2.74	Cit–CH_2 (2bb)	18.7
4	2.68	Cit–CH_2 (ab)	16.3	2.69	Cit–CH_2 (1ab)	16.2
2	2.67	Cit–CH_2 (ba)	14.5	2.68	Cit–CH_2 (1ba)	14.4
12				2.67	Cit–CH_2 (2bb)	18.7
4	2.62	Cit–CH_2 (ab)	16.3	2.63	Cit–CH_2 (1ab)	16.2
2	2.61	Cit–CH_2 (ba)	14.5	2.62	Cit–CH_2 (1ba)	14.4
2	2.54	Cit–CH_2 (bb)	14.5	2.55	Cit–CH_2 (1bb)	14.4
2	2.49	Cit–CH_2 (bb)	14.5	2.49	Cit–CH_2 (1bb)	14.4
9				1.41 (*m*)	inner CH_2 of diaminobutane	
8	1.34 (*m*)	CH_2–CH_2–NH		1.39 (*m*)	inner CH_2 of diaminobutane	

[a]Carbon atom to which protons are bounded, for numbering see Figure 1.

the electrophoretic mobility. Rhizoferrin was transformed into its mono-dehydration product and the mono-dehydration product itself was transformed into a second bis-dehydration product.

Configuration of the ligand

Two chiral centers are present in rhizoferrin which arise from the prochiral quaternary carbon atoms of

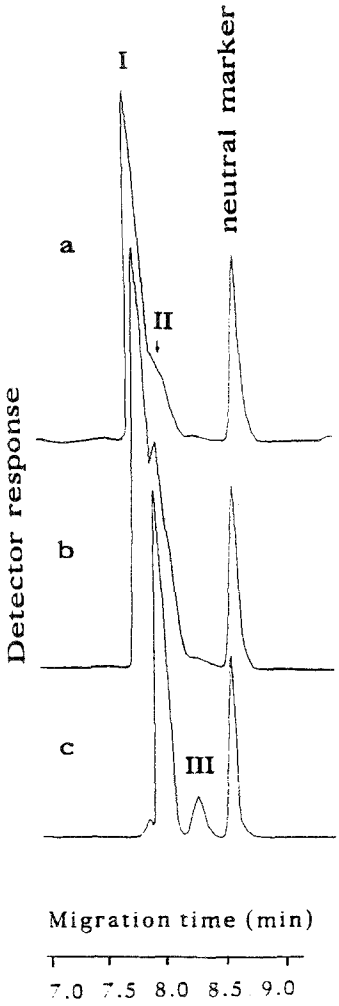

Figure 4. Capillary electrophoretic separation of rhizoferrin (**I**), imidorhizoferrin (**II**) and bis-imidorhizoferrin (**III**). (**a**) Separation of a purified rhizoferrin sample which still contains a small amount of imidorhizoferrin. (**b**) Separation of rhizoferrin after incubation for 1 day in citric acid buffer, pH 2.5 at 25 °C, resulting in an increase of imidorhizoferrin. (**c**) Separation of a sample of imidorhizoferrin after incubation for 1 day in citric acid buffer, pH 2.5, showing residual amounts of rhizoferrin and bis-imidorhizoferrin. For conditions see Materials and methods.

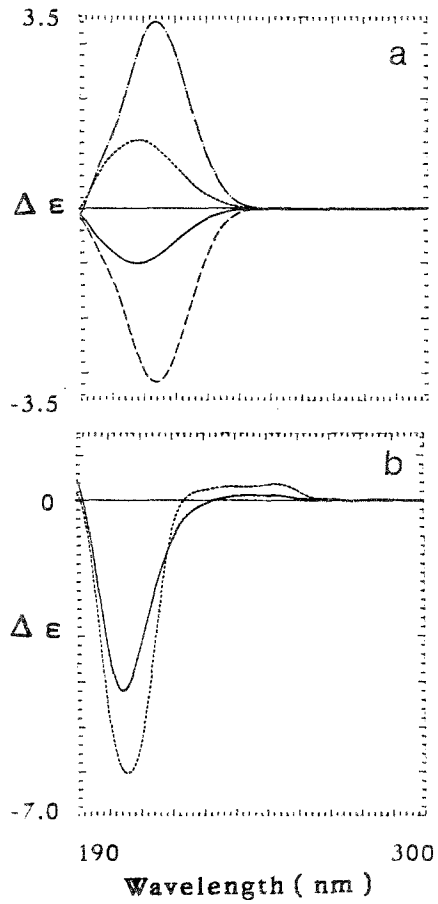

Figure 5. CD spectra of (**a**) upper curves: *S,S*-tartaric acid (– – –) and *S*-malic acid (. . . .); and lower curves *R,R*-tartaric acid (- - -) and *R*-malic acid (—) and (**b**) *R,R*-rhizoferrin (—) and *R,R*-imidorhizoferrin (. . . .).

the citric acid residues after being linked to 1,4-diaminobutane. Thus, the stereochemical configuration of rhizoferrin may be *R,R* or *S,S*, or a meso-form *R,S*. CD measurements at pH 3.0 of the free ligand, rhizoferrin, revealed a single minimum at 204 nm with $\Delta\varepsilon = -4.3$, which precludes a possible *R,S* configuration. Comparisons with *R,R*- and *S,S*-tartaric acid as well as with *R*- and *S*-malic acid (Figure 5a), and with several other chiral hydroxycarboxylic acids, showed that rhizoferrin (Figure 5b) and *R,R*-tartaric acid are analogous in their CD spectra, suggesting that in the natural rhizoferrin both citric acid residues possess the *R,R* configuration. The CD spectra of imidorhizoferrin (Figure 5b) showed the same characteristic minimum at 206 nm with a somewhat higher value for $\Delta\varepsilon = -5.9$ at pH 3.0 ± 0.2 (Figure 5).

UV characterization of the iron complex of rhizoferrin

UV spectra were recorded from mixtures of $FeCl_3 \cdot 6H_2O$ in bidistilled water and stock solutions of rhizoferrin with a stoichiometric ratio of 1:1 and a final concentration of 1.5×10^{-4} M. The pH was varied from 3.0 to 8.7. At pH 3 only a shoulder at 280 nm was found (Figure 6); raising the pH to 4 resulted in a more pronounced expression of a typical charge transfer band at 335 nm and a simultaneous decrease of the shoulder at 280 nm. The charge transfer band reached its maximum at pH 5.5 and a change from pH 6 to 8.7 did not alter

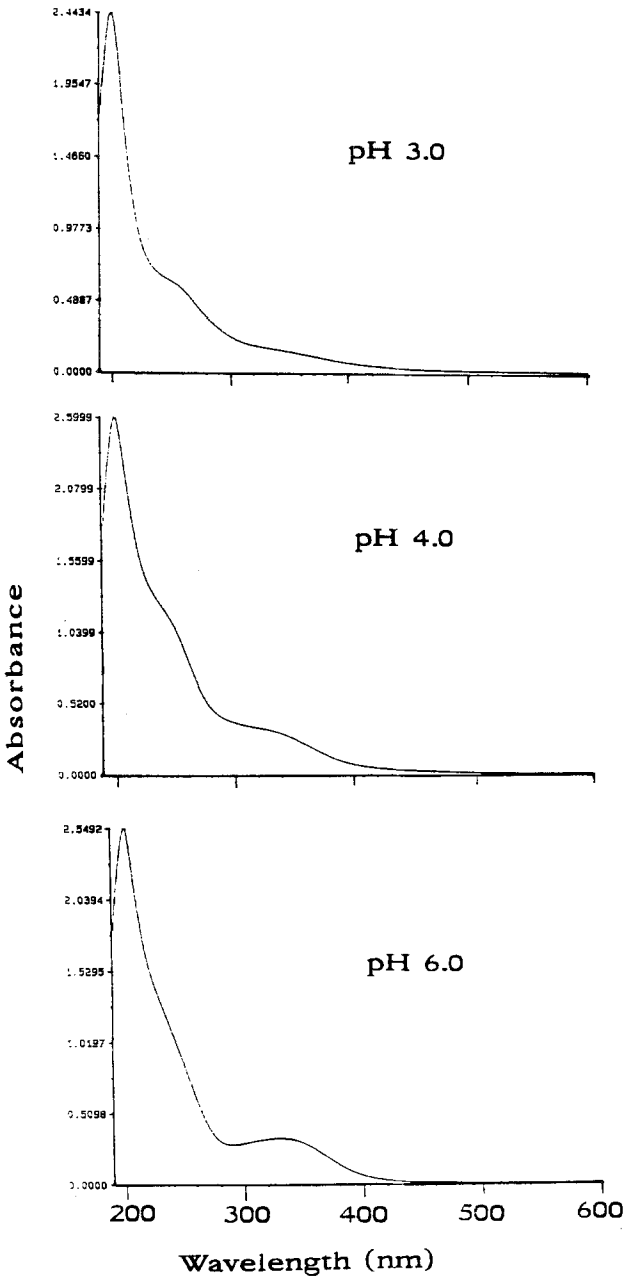

Figure 6. UV spectra of ferric rhizoferrin (1.5×10^{-4} M) at different pH. FTUV, acquisition time 5 s.

the UV spectrum significantly. From this result we inferred that the iron complex of rhizoferrin is completed at pH 5.5–6. Molar extinction coefficients were $\varepsilon = 17\,000\ M^{-1}\,cm^{-1}$ (203 nm, pH 3–9) and $\varepsilon = 2300\ M^{-1}\,cm^{-1}$ (335 nm, pH 6–8).

UV spectroscopy of iron-free rhizoferrin and imidorhizoferrin

The free ligands without addition of iron have been measured in aqueous solution at a concentration of approximately 1.4×10^{-4} M at different pH. The UV absorption band at pH 5.0 (Figure 7) shows a significant bathochromic shift from rhizoferrin (**I**) to the imido form (**II**). The molar extinction coefficients are summarized in Table 3. Rhizoferrin has a maximum at 196 nm, imidorhizoferrin at 202 nm. For a quantitative determination of the purity of isolated samples it is important to note that molar extinction coefficients of rhizoferrin and imidorhizoferrin are comparable only at 200 nm, whereas between 210 and 220 nm the extinction coefficient of imidorhizoferrin is approximately twice as high as that of rhizoferrin.

Configurational studies of the iron complex of rhizoferrin using CD

pH-dependent CD spectra were measured from pH 3.0 to 8.7 at a constant ligand:iron ratio of 1:1 and a concentration of 1.5×10^{-4} M. In a further series (data not shown) the iron:rhizoferrin ratios were changed to 1:4, 2:4, 3:4 and 4:4. As the contours of the spectra did not change with the ratio of iron to

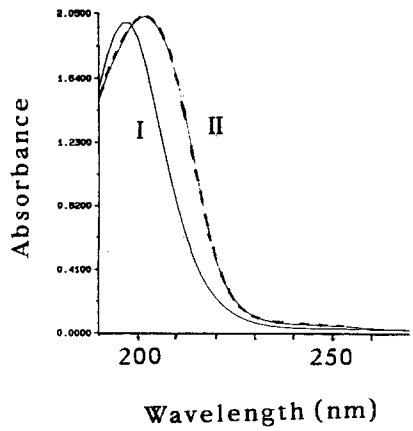

Figure 7. UV spectra of iron-free rhizoferrin (**I**) (1.35×10^{-4} M) and imidorhizoferrin (**II**) (1.42×10^{-4} M). FTUV, acquisition time 25 s, pH 5.0

Table 3. Extinction coefficients ε ($M^{-1}\,cm^{-1}$) of rhizoferrin and imidorhizoferrin

Wavelength (nm)	Rhizoferrin		Imidorhizoferrin	
	pH 3.0	pH 5.0	pH 3.0	pH 5.0
196	13900	14700	13500	14300
200	13150	14000	13300	14200
210	5600	6100	10900	11500
215	3000	3400	6800	7800
220	1400	1700	2700	3300

ligand, we concluded that at pH 5–5.5 no other species than a 1:1 complex of iron to rhizoferrin exists.

CD is generally used as a method of determining ligand chirality about the metal center of siderophores. By comparison with crystal structures of known complexes the absolute configuration of ferric siderophores in solution can be related to the sign of the CD spectra in the region of 300–450 nm. The CD spectra of the pH dependency (Figure 8) changed gradually and their extrema became more pronounced when the pH was raised. While at pH 3.0 characteristic CD absorptions were still absent, positive bands appeared as the pH was gradually increased (Figure 8). The value of $\Delta\varepsilon = 1.9$ compares favorably with the data of ferrichromes (Wong *et al.* 1983). The resulting positive sign of the CD bands between 300 and 450 nm of ferric rhizoferrin indicated that this complex adopts a Λ configuration about the metal center.

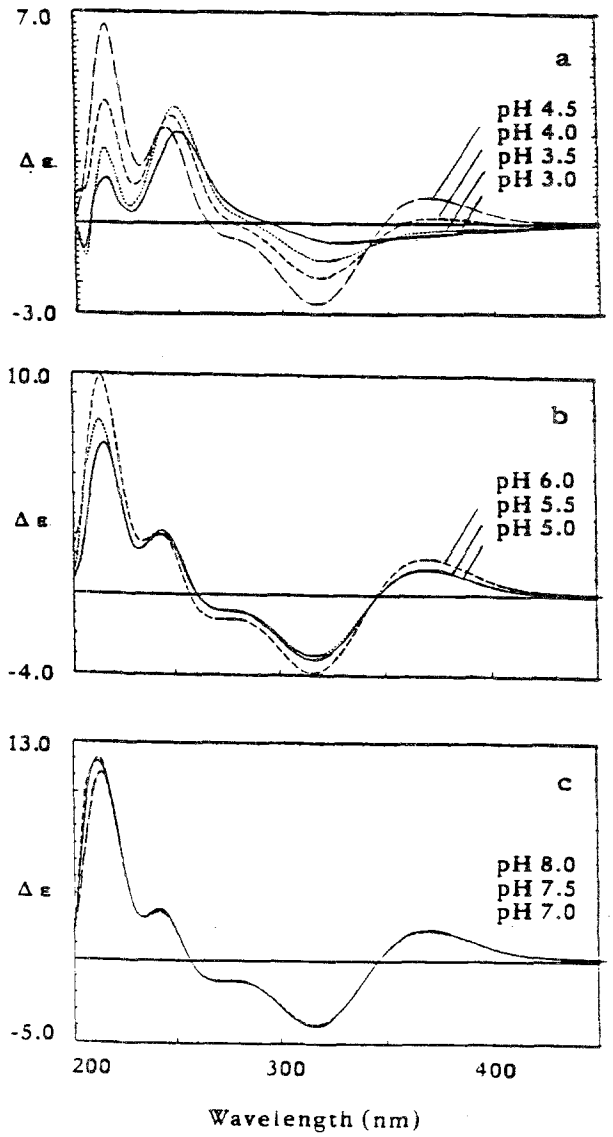

Figure 8. CD spectra of ferric rhizoferrin at different pH.

Characterization of rhizoferrin and imidorhizoferrin by IR spectroscopy

Assignments of the IR spectra for rhizoferrin and imidorhizoferrin (Figure 9) were comparable, with the following differences. The NH valence bands at 3100 cm^{-1} are very weak. The two new CO valence bands at 1770 and 1703 cm^{-1} are typical of five-membered cyclic amides as in the imidoform. The amide **I** band at 1625 cm^{-1} is no longer visible, instead there is a new band at 1640 cm^{-1}; amide **II** is without shift but less intense. The CH deformation bands of the methylene groups at 1443, 1412 and 1376 cm^{-1} show different patterns of intensities. Finally there are several differences of carbon–carbon skeletal vibrations in the fingerprint region.

Discussion

Only a few polycarboxylate or complexone type siderophores have so far been described: rhizobactin and staphyloferrin, isolated from the bacteria *Rhizobium meliloti* (Smith *et al.* 1985) and *Staphylococcus*

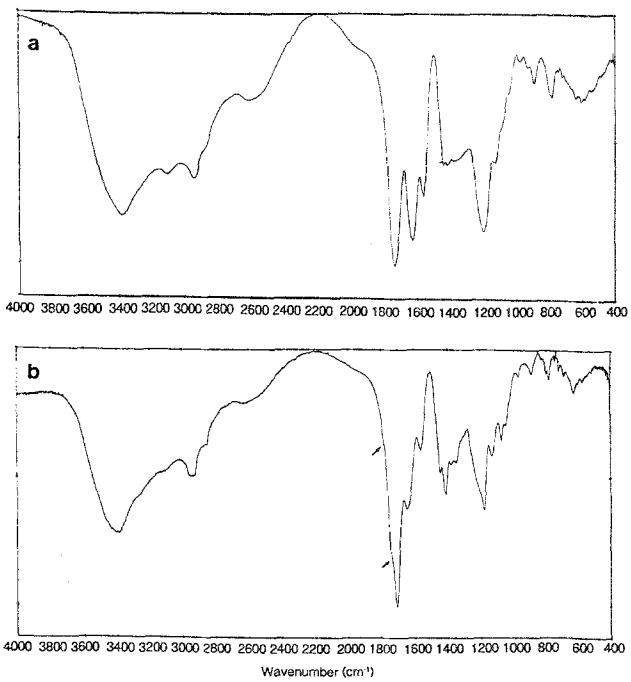

Figure 9. IR spectrum of (**a**) rhizoferrin (**I**) and (**b**) imidorhizoferrin (**II**). KBr pellet, FTIR, 10 scans, resolution 2 cm^{-1}.

hyicus (Konetschny-Rapp *et al.* 1990), respectively, the phytosiderophores of the mugineic acid family isolated from grammineous plants (Nomoto *et al.* 1987) and rhizoferrin isolated from fungi of the Zygomycetes. Thus, polycarboxylate siderophores are distributed in pro- and eucaryotic organisms. Compared with the fungal hydroxamate siderophores possessing high stability constants (Wong *et al.* 1983), the fungal polycarboxylate siderophores seem to have lower stabilities with Fe(III) which may be of relevance to iron removal mechanisms and intracellular storage into ferritins (Winkelmann 1992).

While our previous paper (Drechsel *et al.* 1991) dealt mainly with the structure elucidation of rhizoferrin using ion spray mass spectroscopy and ^{1}H-NMR, the present paper presents further structural and configurational evidence of rhizoferrin and its cyclized dehydration products, named imidorhizoferrin and bis-imidorhizoferrin. ^{13}C-NMR spectroscopy and capillary electrophoresis were used to prove the structures of rhizoferrin and imidorhizoferrin. Moreover, UV and CD spectra revealed a 1:1 ratio and a Λ configuration of the iron complex, and the *R,R* configuration of the quarternary carbon atoms of the two citric acid residues.

Staphyloferrin, a structurally related siderophore isolated from Staphyloccus species, containing D-ornithine instead of putrescin, has also been shown to form two cyclized dehydration products in solution (Konetschny-Rapp *et al.* 1990). The stereochemistry of the citric acid residues in staphyloferrin and the configuration of the iron complex have not yet been unequivocally determined. The present paper provides spectroscopic evidence for a mononuclear ferric–rhizoferrin complex, the Λ-configuration in solution and two citric acid residues with *R,R* configuration. These data are prerequisite for understanding its transport properties in fungi. Further transport studies are in progress to analyze the mechanism of transport of rhizoferrin and its imido forms, and to determine the significance of the stereochemistry during iron transport in fungi. Furthermore, studies on the biochemistry of rhizoferrin are in progress to elucidate the pathway of its stereoselective formation.

Acknowledgments

We thank A. Cansier for expert technical assistance, W. Wassing and B. Saller for recording the IR spectra, and the Deutsche Forschungsgemeinschaft (DFG) for financial support.

References

Drechsel H, Metzger J, Freund S, Jung G, Boelaert JR, Winkelmann G. 1991 Rhizoferrin—a novel siderophore from the fungus *Rhizopus microsporus* var. *rhizopodiformis*. *Biol Met* **4**, 238–243.

Konestchny-Rapp S, Jung G, Meiwes J, Zähner H. 1990 Staphyloferrin A: a structurally new siderophore from staphylococci. *Eur J Biochem* **191**, 65–74.

Nomoto K, Sugiura Y, Takagi S. 1987 Mugineic acids, studies on phytosiderophores. In: Winkelmann G, van der Helm D, Neilands JB, eds. *Iron Transport in Microbes, Plants and Animals*. Weinheim: VCH; 401–425.

Smith MJ, Shoolery NJ, Schwyn B, Holden I, Neilands JB. 1985 Rhizobactin, a structurally novel siderophore from *Rhizobium meliloti*. *J Am Chem Soc* **107**, 1739–1743.

Thieken A, Winkelmann G. 1992 Rhizoferrin—a complexone type siderophore of the Mucorales and Entomophthorales (Zygomycetes). *FEMS Microbiol Lett* **94**, 37–42.

Winkelmann G. 1991 *Handbook of Microbial Iron Chelates*. Boca Raton, FL: CRC Press

Winkelmann G. 1992 Structures and functions of fungal siderophores containing hydroxamate and complexone type iron binding ligands. *Mycol Res* **96**, 529–534.

Wong G, Kappel M, Raymond KN, Matzanke B, Winkelmann G. 1983 Coordination of microbiol iron transport compounds 24. Characterization of coprogen and ferricrocin, two ferric hydroxamate siderophores. *J Am Chem Soc* **105**, 810–815.